*Inorg. Chem.* **2004**, *43*, 27–32


# Exohedral Multiple Bonding in Polyhedra. 2. Skeletal Distortions in Ring-Stacked Boranes

**Musiri M. Balakrishnarajan and Roald Hoffmann***

*Department of Chemistry and Biochemistry, Cornell University, Ithaca, New York 14853*

Received July 28, 2003

Ring-stacked boranes of the $B_{10}H_{10}^{2-}$ and $B_{12}H_{12}^{2-}$ type, when substituted with lone pair bearing groups such as –O, –NH, and –S at the *para* positions, are theoretically shown to exhibit exopolyhedral multiple bonding on oxidation. Successive removal of two and four electrons from the parent $B_nH_{n-2}X_2$ results in highly varied and intriguing skeletal deformations that are explained using fragment molecular theory.

Recently, we suggested that appropriately substituted polyhedral boranes would show *exo*-multiple bonding on oxidation, much like quinones and oxocarbons. This phenomenon was exemplified with the relatively simple octahedral $B_6$ and pentagonal bipyramidal $B_7$ frameworks.[1] Skeletons of higher boranes, such as $B_{10}H_{10}^{2-}$ or $B_{12}H_{12}^{2-}$, are promising targets for nonlinear optical (NLO) materials and molecular switches, as they are reported to show substantial electronic communication across their apical substituents.[2−5] Electronic communication and exohedral multiple bonding are related phenomena, for they both involve the $\pi$-conjugation effect between *para* substituents and the skeletal electrons of the polyhedron. Though bonding in these systems is complex, it can be understood by splitting the molecules into smaller parts and analyzing the nature of interactions between these fragments.[6] Here, we examine whether −O, −NH, and −S substituted $B_{10}$ and $B_{12}$ skeletons might show exohedral multiple bonding upon oxidation.

## 1. Computational Methodology

The fragment MO analysis is performed using extended Hückel calculations.[7] Geometrical optimization of all the systems considered here is done in the framework of hybrid density functional theory (DFT) calculations (B3LYP/6-311+G*) using the Gaussian 98 suite of programs,[8] followed by vibrational analysis to ascertain the nature of stationary points.

## 2. Perturbation of Frontier Orbitals by Exo Substituents

As in the previous study, we begin with a closo polyhedral borane, substituted by two lone-pair bearing ligands X (X= −O, −S, −NH) in the *para* positions. If we deprotonate these (which does not affect their Wadian, closed-shell electronic structure), we come to $B_{10}H_8X_2^{4-}$ and $B_{12}H_{10}X_2^{4-}$. Figure 1 shows the perturbation of frontier molecular orbitals of $B_{12}H_{12}^{2-}$ and $B_{10}H_{10}^{2-}$ on substitution by exo-polyhedral $(O)_2$ $\pi$ orbitals. All the levels shown in the figure are filled in the hypothetical tetraanions.

The 4-fold degenerate HOMO ($g_u$) of icosahedral $B_{12}H_{12}^{2-}$ splits into $e_{1u} + e_{2u}$ upon substitution by oxygen atoms in *para*-$B_{12}H_{10}O_2^{4-}$ (upper left of Figure 1). The $e_{2u}$ set is made up of in-plane p orbitals of the two staggered five-membered rings,[6] and by symmetry remains unaffected by oxygen $\pi$ orbitals. However, the $e_{1u}$ set, made up mainly of the out-of-phase combination of the degenerate $\pi$-MOs of the two

* Corresponding author. E-mail: rh34@cornell.edu.

(1) Balakrishnarajan, M. M.; Hoffmann, R. *Angew. Chem., Int. Ed.*, in press.
(2) Kaszynski, P.; Doughlass, A. G. *J. Organomet. Chem.* **1999**, *581*, 28.
(3) Knoth, W. H. *J. Am. Chem. Soc.* **1966**, *88*, 935.
(4) Kaszynski, P.; Huang, J.; Jenkins, G. S.; Bairamov, K. A.; Lipiak, D. *Mol. Cryst. Liq. Cryst.* **1995**, *260*, 315.
(5) Fox, M. A.; Macbride, J. A. H.; Peace, R. J.; Wade, K. *J. Chem. Soc., Dalton Trans.* **1998**, 401.
(6) Balakrishnarajan, M. M.; Hoffmann, R. Pancharatna, P. D.; Jemmis, E. D. *Inorg. Chem.* **2003**, *42*, 4650.
(7) (a) Hoffmann, R.; Lipscomb, W. N. *J. Chem. Phys.* **1962**, *36*, 2179. (b) Hoffmann, R. *J. Chem. Phys.* **1963**, *39*, 1397.
(8) Frisch, M. J.; Trucks, G. W.; Schelegel, H. B.; Gill, P. M. W.; Johnson, B. G.; Robb, M. A.; Cheeseman, J. R.; Keith, T.; Peterson, G. A.; Montgomery, J. A.; Raghavachari, K.; Al-Laham, M. A.; Zakrzewski, V. G.; Oritz, J. V.; Foresman, J. B.; Cioslowsky, J.; Stefenov, B. B.; Nanayakkara, A.; Callacombe, M.; Peng, C. Y.; Ayala, P. Y.; Chen, W.; Wong, M. W.; Andres, J. L.; Replogle, E. S.; Gomberts, R.; Martin, R. L.; Fox, D. J.; Binkley, J. S.; Defrees, D. J.; Baker, J.; Stewart, J. P.; Head-Gordon, M.; Gonzalez, C.; Pople, J. A. *Gaussian 98*, version 5.2; Gaussian Inc.: Pittsburgh, PA, 1995. B3LYP is Becke's three parameter hybrid method with LYP correlation functional: (a) Becke, A. D. *J. Chem. Phys.* **1993**, *98*, 5648. (b) Lee, C.; Yang, W.; Parr, R. G. *Phys. Rev. B* **1988**, *37*, 785. (c) Vosko, S. H.; Wilk, L.; Nusair, M. *Can. J. Phys.* **1980**, *58*, 1200. (d) Stephens, P. J.; Delvin, F. J.; Chabalowski, C. F.; Frisch, M. J. *J. Phys. Chem.* **1994**, *98*, 11623.

10.1021/ic034891y CCC: $27.50 
Published on Web 12/10/2003

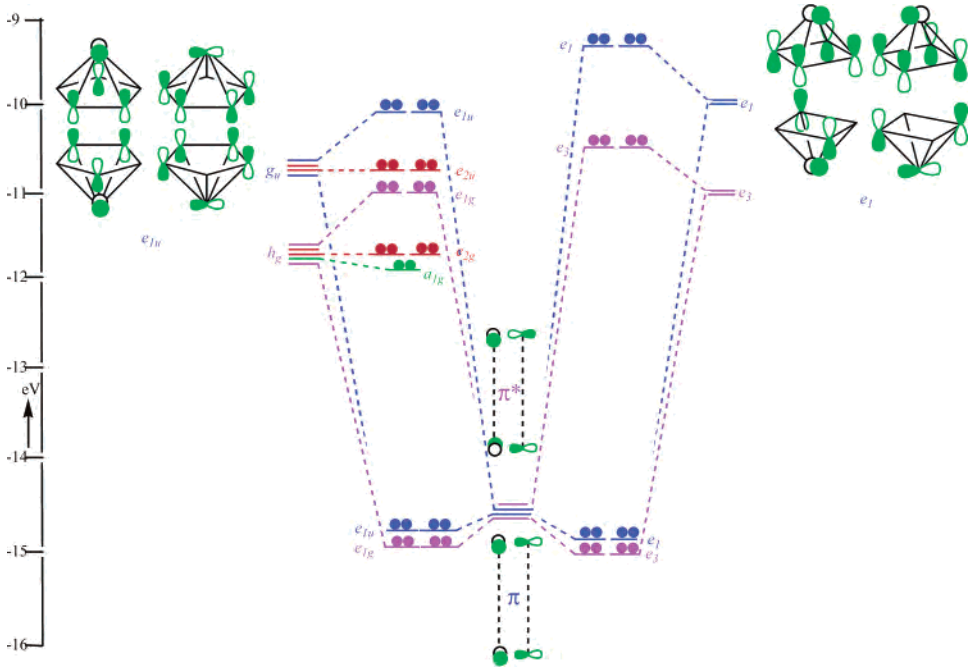


**Figure 1.** The perturbation of the frontier MOs of $B_{12}H_{12}^{2-}$ ($I_h$, left) and $B_{10}H_{10}^{2-}$ ($D_{4d}$, right) by the substitution of the two apical hydrogens with two oxygen atoms (in the middle), leading to the occupied MOs of *closo*-$B_{12}H_{10}O_2^{4-}$ ($D_{5d}$) and *closo*-$B_{10}H_8O_2^{4-}$ ($D_{4d}$). Only the essential high-lying MOs are shown.

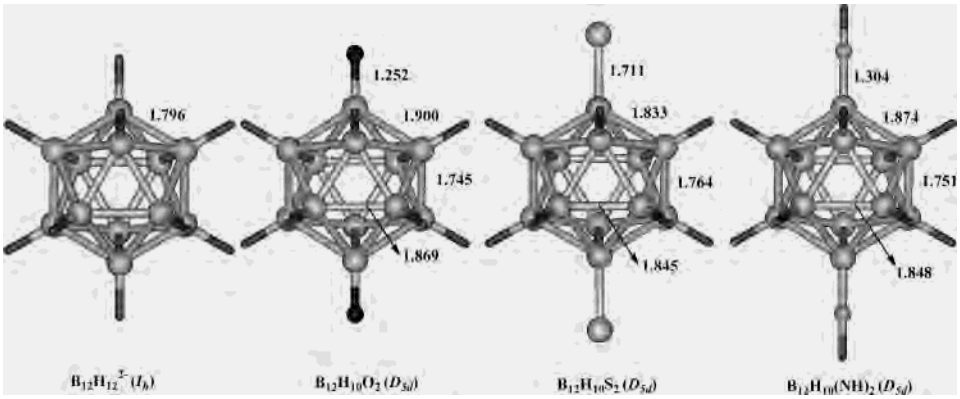


**Figure 2.** $B_{12}H_{12}^{2-}$ and *closo*-$B_{12}H_{10}X_2$ systems having *exo*-multiple bonds, with their bond lengths (in Å) calculated at the B3LYP/6-311+G** level of theory.

staggered *nido*-$B_6H_5$ fragments (each resembling the HOMO of $C_5H_5^-$), has the right symmetry to interact with the in-phase combination ($\pi_u$) of $(O)_2$. The result is a pair of bonding and antibonding MOs (indicated in Figure 1). The latter form the HOMO of $B_{12}H_{10}O_2^{4-}$.

For $B_{10}H_{10}^{2-}$ ($D_{4d}$), the HOMO is only doubly degenerate ($e_1$); the orbitals here arise from the out-of-phase combination of the degenerate $\pi$-MOs of the two staggered *nido*-$B_5H_4$ fragments (resembling the HOMO of $C_4H_4^{2-}$). They mix strongly with the in-phase combination of the ($O_2$) $\pi$ orbitals—the antibonding combination forming the HOMO of $B_{10}H_8O_2^{4-}$. These interactions are very similar to those observed in the $B_6$ and $B_7$ systems,[1] except for the change in phase of the oxygen $\pi$ orbitals that interact with the HOMO.

On oxidation, electrons have to be removed from the doubly degenerate HOMO of these $B_nH_{n-2}X_2^{4-}$ systems. In every case, the HOMO—the out-of-phase combination of polyhedron tangential orbitals and the oxygen p orbitals—is antibonding in the B−X region. Hence, removal of four or two electrons from this HOMO will result in the exohedral B−X multiple bonding that is described in detail in the subsequent sections.

### 3. Neutral $B_nH_{n-2}X_2$ Systems

**3.1. $B_{12}H_{10}X_2$.** Removal of four electrons from the parent tetraanion ($B_nH_nX_2^{4-}$) is not likely to affect the symmetry of this system, as another closed-shell molecule is reached (Figure 1). However, such oxidation should shorten the B−X distances dramatically. This is exactly what is observed—compare for instance the calculated distances for $B_{12}H_{10}X_2$ (X = O, S, and NH) in Figure 2 with B−X bond lengths in experimentally known compounds: B−O = 1.480 Å ($B_{12}H_{11}OH^{2-}$), B−S = 1.862 Å ($B_{12}H_{11}SH^{2-}$), B−N = 1.521 Å ($B_{12}H_{11}$ $[NH_3]^{-1}$).[9] All the $B_{12}H_{10}X_2$ (X = O, S, NH) were

(9) Sivaev, I. B.; Bregadze, V. I.; SjÖberg, S. *Collect. Czech. Chem. Commun.* **2002**, *67*, 679.

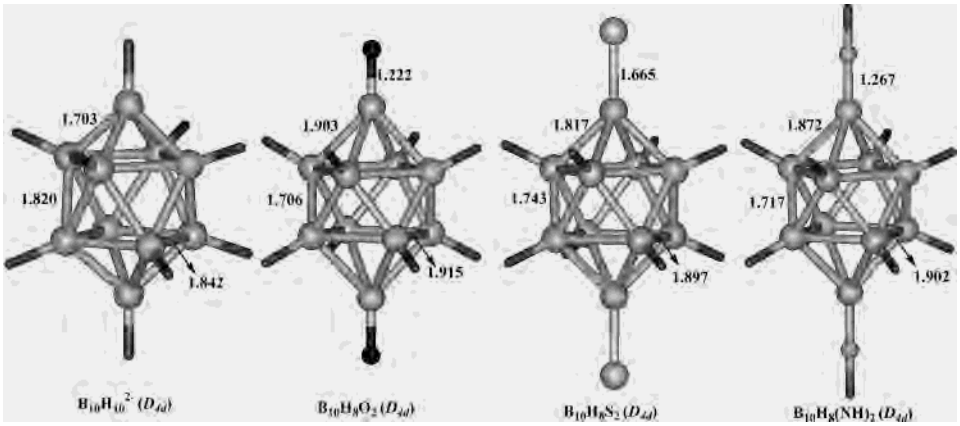


**Figure 3.** $B_{10}H_{10}^{2-}$ and *closo*-$B_{10}H_8X_2$ systems having *exo*-multiple bonds, with their bond lengths (in Å) calculated at the B3LYP/6-311+G** level of theory.

optimized within a $D_{5d}$ symmetry constraint and characterized as stationary points.

On going from the tetraanion to the neutral species, electrons are also removed from an MO that is net bonding between all the adjacent boron atoms of the $B_{12}$ cage. Hence we expect the entire cage to expand. The optimized geometries of all these systems show pronounced and uniform bond-length elongations in their skeletons as expected, except for the inter-ring bonds (central girdle), which are shortened. We do not yet understand the reasons for this shortening.

All B−B distances, even the quite longer ones, are well within the range of standard polyhedral B−B distances, observed experimentally. The extent of skeletal deformation increases with increasing electronegativity of the substituents, the −O substituent showing the maximum deformation, followed by −NH and −S. In the −NH substituted systems, the B−N−H fragment stays linear, indicating a cylindrical B≡N type of interaction.

**3.2. $B_{10}H_8X_2$.** A similar substitution sequence in the *closo*-$B_{10}$ skeleton was optimized within a $D_{4d}$ symmetry constraint, and every molecule is characterized as a stationary point. The various bond distances calculated are given in Figure 3.

As in the case of the $B_{12}$ skeleton, since the electrons are removed from a doubly degenerate HOMO which is bonding everywhere in the polyhedron, one would expect that the corresponding B−B bonds are elongated with respect to the unsubstituted $B_{10}H_{10}^{2-}$ skeleton. They are, except for the inter-ring B−B bonds of the central girdle, which are shortened. These geometric trends are observed consistently for all the substituents considered here, the effects being more pronounced for −O, followed by −NH and −S. The B−X distances show trends similar to those calculated for the $B_{12}$ skeleton, the shortening more pronounced in the $B_{10}$ skeleton. This accords with earlier assertions that the $B_{10}$ skeleton has a greater propensity to exhibit $\pi$-conjugation than the $B_{12}$ skeleton.[2]

## 4. Dianionic $B_nH_{n-2}X_2^{2-}$ Systems

Removal of just two electrons from the parent tetraanions ($B_nH_nX_2^{4-}$) is expected to have a major effect on the symmetry of these systems. Since the doubly degenerate HOMO is then partially occupied, with two electrons in both cases, we have a classic Jahn−Teller system. A distortion lifting the degeneracy should follow.

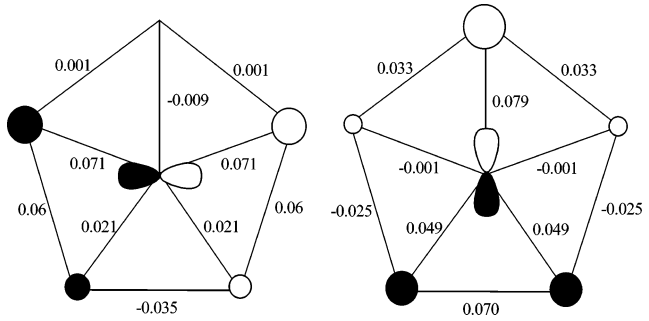


**Figure 4.** The coefficients (schematic solid and open circles) and overlap populations between the boron atoms in the $B_6H_5O^{2-}$ fragment due to occupation of a single electron in each of the doubly degenerate HOMO. The view is along the $C_5$ axis.

Initial DFT calculations carried out at the B3LYP/6-311+G* level of theory had geometrical convergence problems. Unlike the case of mono-ring cages such as $B_6$ and $B_7$, in these $B_{10}$ and $B_{12}$ stacked ring systems there are several possible distortions that will break the degeneracy of the doubly degenerate MOs. We suspected that the convergence problems might be due to the complicated nature of the Jahn−Teller potential energy surface. So we took a qualitative look at the MOs involved, and how they might change upon deformation.

**4.1. $B_{12}H_{10}X_2^{2-}$.** To understand the nature of Jahn−Teller distortion in the $B_{12}H_{10}X_2^{2-}$ ($D_{5d}$) cage, we divide its *closo* skeleton into two equal $B_6H_5X^-$ ($C_{5v}$) fragments. Consider such an odd-electron *nido*-$B_6H_5O^{2-}$ ($C_{5v}$) fragment. The schematic shape of the degenerate HOMO set (from an extended Hückel calculation) is shown in Figure 4. The overlap population between the boron atoms, due to occupation of one of these orbitals by a single electron, is also shown in Figure 4. In the composite $B_{12}$ skeleton, the MOs that are shown in Figure 4 or 5 will interact with their counterparts in the other fragment.

These orbital patterns suggest two quite different distortions: (1) one in which the B−B bond lengths around the ring alternate shorter, longer, shorter, unaffected, unaffected

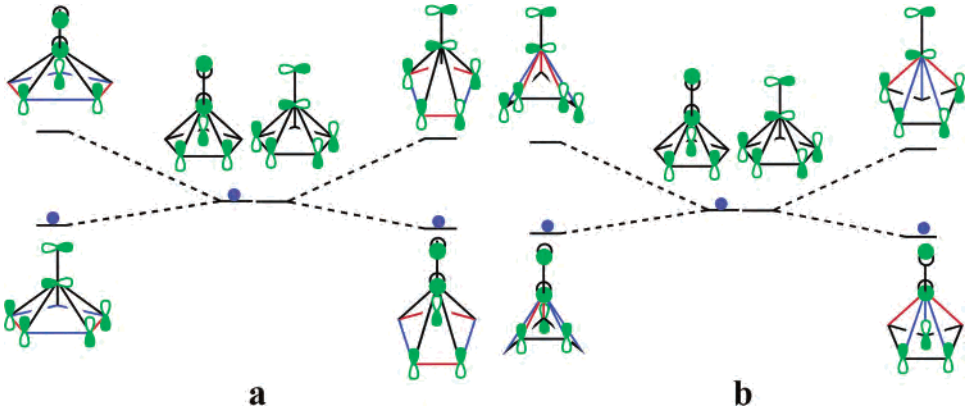


**Figure 5.** Two possible ways of in-plane distortion in the $B_6H_5X^{-2}$ fragment due to occupation of the doubly degenerate HOMO by a single electron. The short bonds are shown in red and long ones in blue.

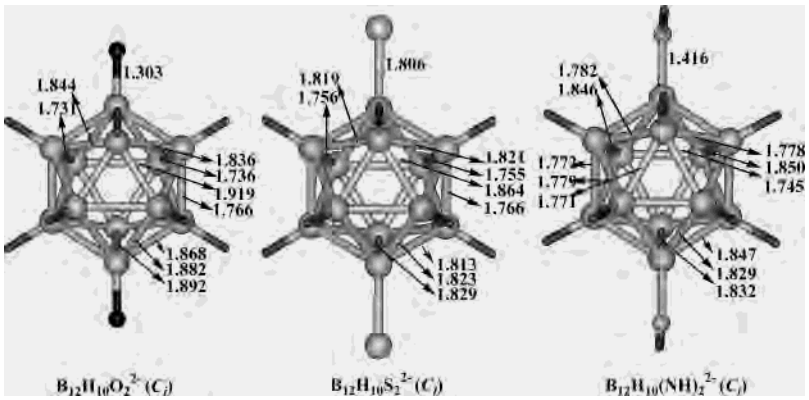


**Figure 6.** *closo*-$B_{10}H_8X_2^{2-}$ systems having *exo*-multiple bonds, with their bond lengths (in Å) calculated at the B3LYP/6-311+G** level of theory.

around the ring; (2) another in which the bond length pattern is long, very short, long, medium short, medium short around. Moreover, the substantial and different cap-ring OPs suggest that out-of-plane distortions of the five-membered ring might also happen. All these distortions reduce the $C_{5v}$ symmetry of the $B_6H_5X$ fragment to $C_{2v}$, as illustrated in Figure 5.

Guided by this analysis, we were led to converged structures of the dianions with severely distorted geometries. The geometries (Figure 6) reflect the trends outlined above, remarkably choosing one or another of the possible stabilizing distortions. For instance, for −O and −S substituted systems, geometry optimizations within a $C_{2h}$ symmetry constraint lead to small imaginary frequencies and a local minimum with reduced $C_i$ symmetry. In both cases, the $B_5$ rings of the optimized geometries exhibit substantial bond alternation, having two short, two long, and one very long bonds.

Amazingly, in $B_{12}H_{10}(NH)_2^{2-}$ the pentagonal rings are computed to deform in an alternative way, having two long, two short, and one very short bonds. Further, the planarity of both the $B_5$ rings is destroyed to a smaller extent (within 0.03 Å) in all these systems, indicating that both in-plane and out-of-plane distortions occur concurrently. The in-plane distortion (Figure 5a) is more pronounced than the out-of-plane distortion (Figure 5b) for all substituents. The B−X bonds of these systems lie between typical B−X single bonds and the B−X bonds of the neutral $B_{12}H_{10}X_2$ systems. In the −NH substituted systems, the B−N−H fragment bends, indicating a B═N type of interaction.

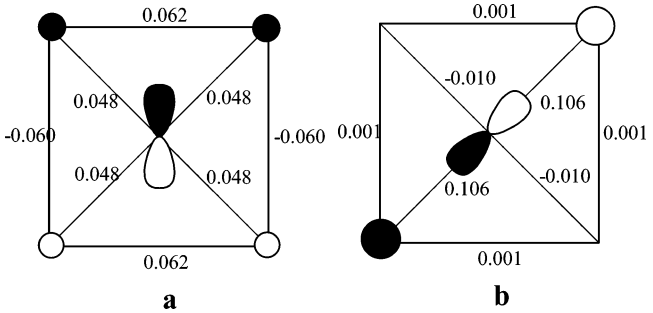


**Figure 7.** The overlap population between the boron atoms in the $B_5H_4X$ fragment viewed along the $C_4$ axis, due to occupation of a single electron in the doubly degenerate HOMO, in two different representations.

**4.2. $B_{10}H_8X_2^{2-}$.** The Jahn−Teller distortion in the dianionic $B_{10}H_8X_2^{2-}$ systems can be analogously analyzed by fragmenting into $B_5H_4X$ fragments. An extended Hückel calculation on *nido*-$B_5H_4O^{2-}$ ($C_{4v}$) leads to a doubly degenerate HOMO that is singly occupied as expected. The doubly degenerate MO can be represented in two different ways, as indicated in Figure 7 left and right. Since each representation is associated with a different possible deformation, let us look at the overlap population trends accompanying occupation of each orbital.

The in-plane distortion favored by the combination shown in Figure 7a is likely to lead to two short and two long bonds alternating in the $B_4$ ring (Figure 8a), whereas the out-of-plane distortion implied by the orbital choice Figure 7b entails a butterflylike geometry (Figure 8b). Both these

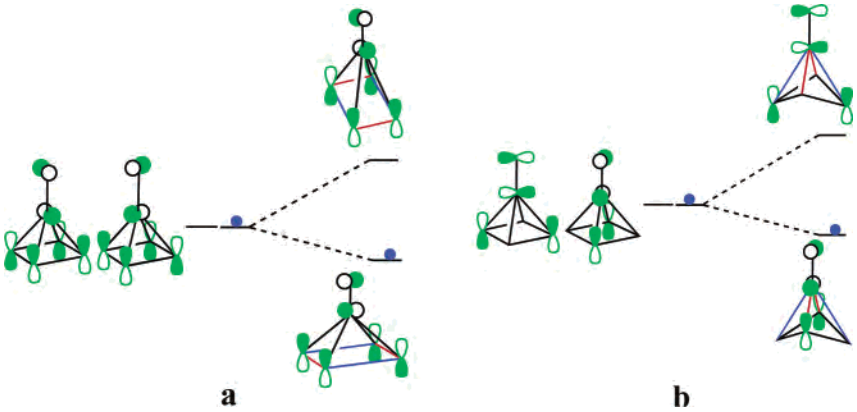


**Figure 8.** Two possible ways of in-plane distortion in the $B_5H_4X^{-2}$ fragment due to occupation of the doubly degenerate HOMO by a single electron. The short bonds are shown in red and long ones in blue.

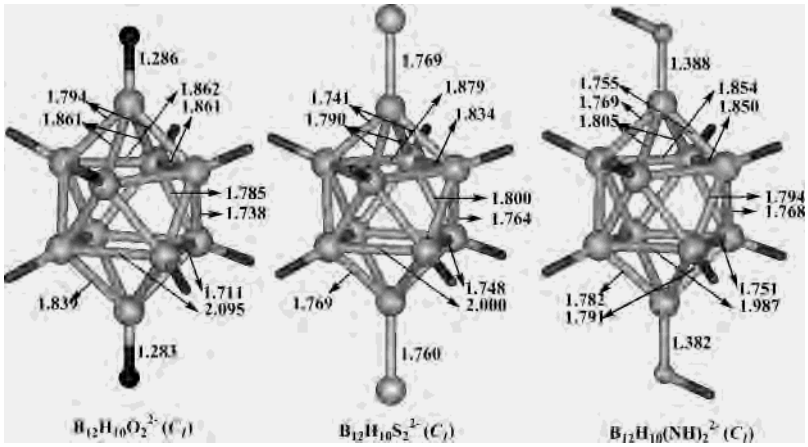


**Figure 9.** *closo*-$B_{10}H_8X_2^{2-}$ systems having *exo*-multiple bonds, with their bond lengths (in Å) calculated at the B3LYP/6-311+G** level of theory.

distortions reduce the $C_{4v}$ symmetry of the $B_5H_4X$ fragment to $C_{2v}$.

Remarkably, the optimized geometries of all the $B_{10}H_8X_2^{2-}$ systems considered have one of the $B_4$ rings showing an in-plane distortion, while the other $B_4$ ring is subject to an out-of-plane deformation (Figure 9. The ideal $C_{2v}$ geometry has a small imaginary frequency, distorting it to a $C_1$ minimum.

The richness and complexity of Jahn−Teller distortions in these systems is obvious. It will take a very careful analysis to pin down the static and dynamic nature of the geometries of these molecules, when they are made.

The B−X bond distances in the dianions are slightly elongated compared to the neutral $B_{10}H_8X_2$ systems, presumably due to the diminution of $\pi$-bonding. In comparison to the dianionic $B_{12}$ derivatives, the B−X bonds are uniformly shorter, similar to the trends observed in the neutral systems. These distortions are more pronounced with −O, followed by −S and −NH, as in the case of the multiply bonded $B_{12}H_{10}X_2$ systems described earlier.

## 5. Oxocarbon Analogues

The icosahedral $B_{12}$ cage is also capable of exhibiting multiple bonding similar to that in oxocarbon dianions, as indicated earlier for $B_6X_6^{2-}$ systems. There are several Wadian closomers reported in which all the 12 hydrogen positions of the $B_{12}H_{12}^{2-}$ are functionalized.[10] The isolation of neutral compounds such as $B_{12}Cl_{12}$ and $B_{12}(OCH_2C_6H_5)_{12}$ indicates that the substituted $B_{12}$ cage is amenable to oxidation.[11,12]

In a hypothetical Wade system $B_{12}O_{12}^{14-}$ (take $B_{12}H_{12}^{2-}$ on paper to $B_{12}(OH)_{12}^{2-}$ to $B_{12}O_{12}^{14-} + 12H^+$) the 24 $\pi$ type orbitals of the 12 external O substituents transform as $h_g + 2g_g + g_u + t_{1u} + t_{2g} + a_g$. Of these, $g_u$, the HOMO in the classical icosahedral framework, interacts strongly with the corresponding symmetry oxygen lone pair combinations, as illustrated schematically in Figure 10.

A good HOMO−LUMO gap results if this framework-oxygen antibonding combination is unfilled. This implies an eight-electron oxidation of $B_{12}O_{12}^{14-}$ to $B_{12}O_{12}^{6-}$. The 6− charge is rather high, but the next closed-shell structure is at $B_{12}O_{12}^{4+}$, which is electron deficient. For either case, removal of electrons leads to exopolyhedral $\pi$-bonding.

DFT calculations on $B_{12}O_{12}^{6-}$ ($O_h$) and $B_{12}S_{12}^{6-}$ ($O_h$) show that these oxygenated borates are indeed minima on their

(10) (a) Muetterties, E. L.; Knoth, W. H. *Polyhedral Boranes*; Marcel Dekker: New York, 1968. (b) Peynmann, T.; Knobler, C. B.; Hawthorne, M. F. *Inorg. Chem.* **2000**, *39*, 1163. (c) Peynmann, T.; Knobler, C. B.; Khan, S. I.; Hawthorne, M. F. *J. Am. Chem. Soc.* **2001**, *123*, 2182. (d) Peynmann, T.; Knobler, C. B.; Khan, S. I.; Hawthorne, M. F. *Inorg. Chem.* **2001**, *40*, 1291. (e) Thomas, J.; Hawthorne, M. F. *Chem. Commun.* **2001**, 1884. (f) Maderna, A.; Knobler, C. B.; Hawthorne, M. F. *Angew. Chem., Int. Ed.* **2001**, *40*, 1661.
(11) Morrison, J. A. *Chem. Rev.* **1991**, *91*, 35.
(12) Peymann, T.; Knobler, C. B.; Khan, S. I.; Hawthorne, M. F. *Angew. Chem., Int. Ed.* **2001**, *40*, 1664.

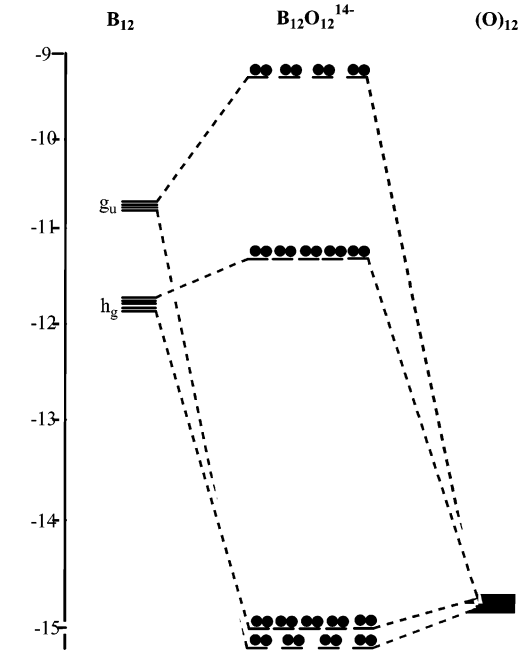


**Figure 10.** The interaction of a $B_{12}$ ($I_h$) fragment with 12 oxygen atoms ($I_h$), resulting in the bonding MOs of *closo*-$B_{12}O_{12}^{14-}$. Just a selection of the framework orbitals near the HOMO, and of the 24 oxygen $\pi$ orbitals is shown.

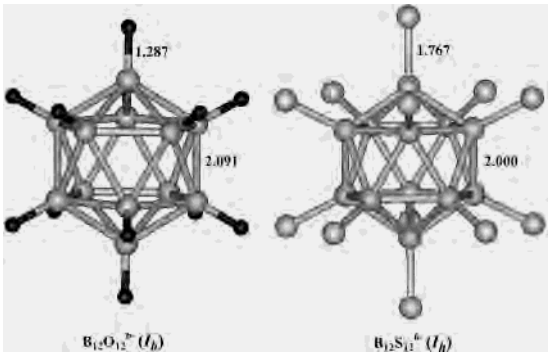


**Figure 11.** *closo*-$B_{12}X_{12}^{6-}$ systems having *exo*-multiple bonds, with bond lengths (in Å) as calculated at the B3LYP/6-311+G** level of theory.

potential energy surface (Figure 11) retaining their icosahedral symmetry. The B−B bond lengths are substantially elongated (up to 2.09 Å), which is partially due to the higher negative charge (Figure 11). The B−X bonds also are short compared to typical B−X single bond distances. Since these systems show good HOMO−LUMO gaps, they may possibly exist in the solid state, as Zintl ions, if not in solution. Substitution of some of the boron atoms by carbon can also help in alleviating the high negative charge.

Recently, Maderna et al.[10f] have synthesized $B_{12}(OCH_2Ph)_{12}^{2-}$; this molecule was also reported to undergo oxidation by one and two electrons to stable compounds.[11] The structures of the Wadian dianion and the neutral (called *hypercloso*) were determined. There is an interesting relationship between the systems we propose in this contribution and the synthesized $B_{12}(OCH_2Ph)_{12}$. Were the B−O−$CH_2$-Ph linkages linear at O, $B_{12}(OCH_2Ph)_{12}^{2-}$ could be viewed as $B_{12}O_{12}^{14-}$ + 12 $^+CH_2Ph$. The bending at oxygen complicates things a little, but not essentially—$B_{12}(OCH_2Ph)_{12}^{2-}$ is like $B_{12}O_{12}^{14-}$. The neutral system (see Figure 10) would have $g_u$ occupied by six electrons, should show signs of multiple B−O bonding, and will also be subject to a Jahn−Teller deformation. The geometric consequences were indeed observed in the X-ray structure of $B_{12}(OCH_2C_2H_5)_{12}$.[12,13] There is a substantial deformation of the $B_{12}$ cage to approximate $D_{3d}$ symmetry on oxidation. Further, the B−O bonds are shortened by ∼0.06 Å relative to the dianion.

The range of possibilities available for polyhedral boranes with exohedral multiple bonding parallels the diverse chemistry of organic aromatic systems with exocyclic double bonds.

**Acknowledgment.** We are grateful to the National Science Foundation for its support of this research through Grant CHE -0204841.

**Supporting Information Available:** Optimized Cartesian coordinates of various substituted boranes and their total energies. This material is available free of charge via the Internet at http://pubs.acs.org.

IC034891Y

(13) See also the theoretical studies on the oxidation of $B_{12}H_{12}^{2-}$ and $B_{12}X_{12}^{2-}$. (a) McKee, M. *Inorg. Chem.* **2002**, *41*, 1299. (b) Fujimori, F.; Kimura, K. *J. Solid State Chem.* **1997**, *133*, 178.